Long-term Survival Results following Endobronchial RF Ablation in a Healthy-Porcine Model

K. Y. Yoneda, MD, F. Herth, MD, T. Spangler, DVM, S. Raina, PhD, and D. Panescu, PhD, *Fellow IEEE*

***Abstract*—This paper presents results from long-term survival study where healthy swine were ablated with a novel technology designed for treating early-stage non-small cell lung cancer using an endobronchial flexible catheter.**

Methods — The radiofrequency ablation (RFA) system has been presented previously and consisted of an ablation catheter, radiofrequency generator, irrigation pump for infusion of hypertonic saline (HS) and a laptop. The catheter carried an occlusion balloon, a 5 mm long RF electrode, with irrigation holes, and a 1 mm long electrode for bipolar impedance measurements. The outer diameter (OD) was 1.4 mm for compatibility with current bronchoscopes, navigation systems and radial EBUS. Nine swine were treated in this study with survival times of 1, 4 and 12 weeks (N=3 at each time point). In all animals, the treatment sites consisted of one location in the upper right lung (RUL) and another one in the lower right lung (RLL). CTs were taken pre-op, immediately post-op and at every 2 weeks post treatment. Ablation times ranged from 6 to 8 min and average applied power was 68 W (range 63 – 72 W).

Results — At 1-week survival, large zones of necrotic tissue were observed in all respective 6 ablations. Ablation volumes had an average diameter of 3.2 cm at RUL locations and 3.8 cm in RLLs (likely due to longer RLL ablation durations). As time progressed, the necrotic tissue was gradually replaced with fibrotic tissue. At 4-week survival, the replacement was almost complete in all respective 3 animals. As a result, ablation volumes decreased to an average diameter of 1.3 cm at RUL locations and 2.3 cm in RLLs (likely due to longer RLL ablation durations). At 12-week survival, as the replacement process continued, histopathology revealed zones of residual necrotic tissue that were further reduced in size. Ablation zones had been resorbed and contracted by fibrous scar tissue. The average volume of the treatment effect decreased to 1.1 cm (RUL) and to 1.6 cm (RLL) in equivalent diameter. There were no complications in any of the nine animals.

Conclusion — In healthy swine lungs, RFA with a 1.4-mm OD, radial-EBUS-sheath-compatible, endobronchial catheter was effective and safe. This system and therapeutic approach may be considered for further evaluation in minimally invasive treatment of tumorous lung nodules.

Keywords: **Ablation, Cancer, Catheter, Endobronchial, Radiofrequency.**

I. Introduction

Lung cancer is the most common cancer in the world with over two million cases diagnosed every year [1]. Surgical resection is considered the best treatment for long term survival of patients with non-small cell lung cancer (NSCLC). However, patients with comorbidities or of advanced age may not be suitable candidates for resection [2]. According to Chen et al., medically inoperable patients account for 85% of all lung cancer patients [3]. Less invasive therapies are used for such non-surgical candidates with early-stage disease. Radiofrequency Ablation (RFA) is one such therapy that uses oscillating electrical fields to heat up the site of the tumor and cause necrosis of the tumor cells [4 – 8]. We have previously presented early preclinical data with a novel endobronchial RFA system designed for treatment of lung cancer [9]. Our present goal was to follow up on our previous experience and report the findings of a 12-week survival healthy-swine study.

II. Methods

A. RFA System

Although we have previously described our novel RFA system, we will provide another summary of its features [9]. As shown in Fig. 1, its main components were: an ablation catheter, a radiofrequency generator (RFG), an irrigation pump (IP) and a laptop. The generator was a monopolar RFG platform utilizing a catheter equipped with two electrodes: a 5 mm long RF electrode with holes for irrigation with hypertonic saline (HS) by the irrigation pump and a 1 mm long electrode used for bipolar impedance measurements. The cross-sectional diameter of the catheter was 1.4 mm. It ensured compatibility with working channels of existing bronchoscopes, navigation systems and with radial EBUS guide sheaths. The impedance electrode was used to measure the bipolar impedance before RF energy is applied. The catheter had a silicone balloon with a maximum diameter of 12 mm when inflated. This balloon helped anchor the RF electrode in the targeted bronchus during ablation and also confined the HS flow to the intended treatment area. The laptop provided the user interface for control and monitoring.

In this study, we used, mostly, HS with a concentration of 23.4% [11]. The catheter was connected to the generator through a catheter cable. The generator supported one channel of monopolar RF power delivery to a neutral return electrode. Hypertonic saline was used to enhance the contact between airway wall and electrode [2, 8]. Due to its increased electrical conductivity, HS provided for a larger 'virtual' electrode. Previous studies indicated increased ablation volumes when HS concentrations greater than 5% were used [2, 4, 8].

Dr. K. Y. Yoneda is Professor Pulmonology, UC Davis, CA 95616, USA.
Dr. F. Herth is Professor, Chair, Pneumology and Critical Care Medicine, Thoraxklinik, University of Heidelberg, Germany.
Dr. T. Spangler is Pathologist at VDx Preclinical Research Services, Davis CA 95616, USA.
Dr. S. Raina is with Zidan Medical, Inc., Santa Clara, CA 95051, USA.
Dr. D. Panescu is with Zidan Medical, Inc., Santa Clara, CA 95051, USA (e-mail dpanescu@coridea.com).

Figure 1. Configuration of the RFA system used in this study.

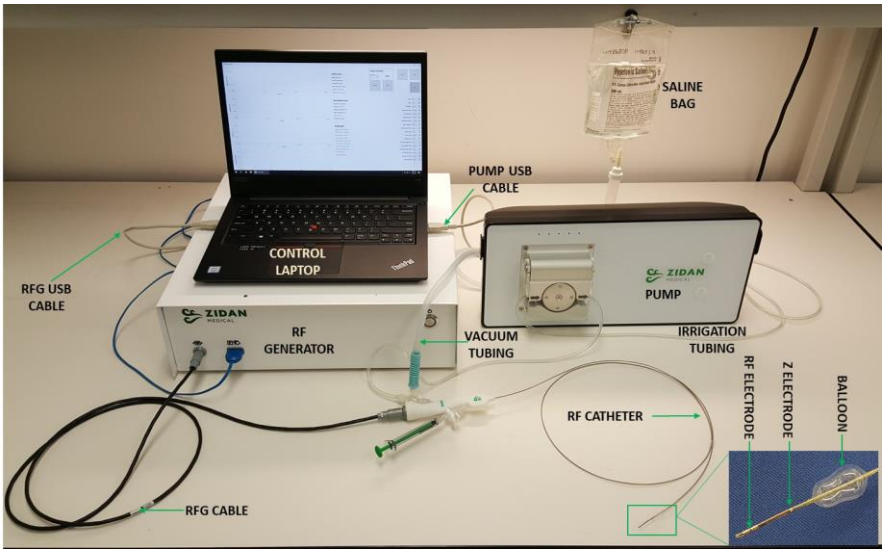

Figure 2. Detailed view of the distal end of the RFA catheter.

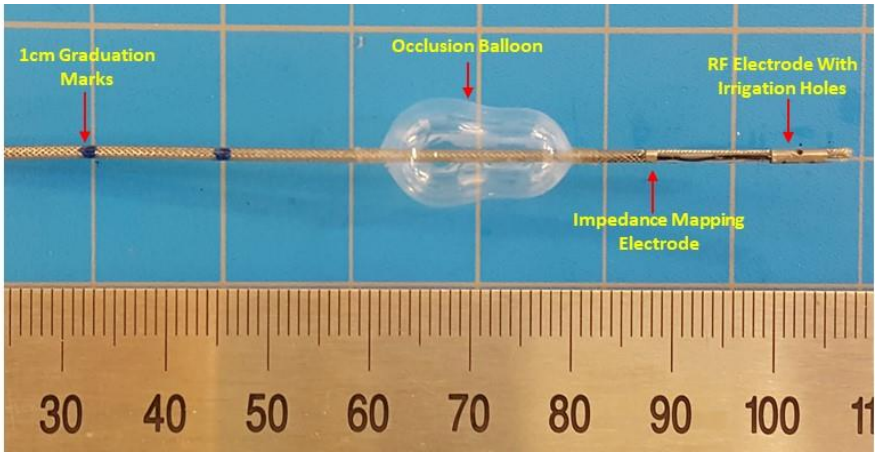

Figure 3. Catheter deployment through a standard bronchoscope.

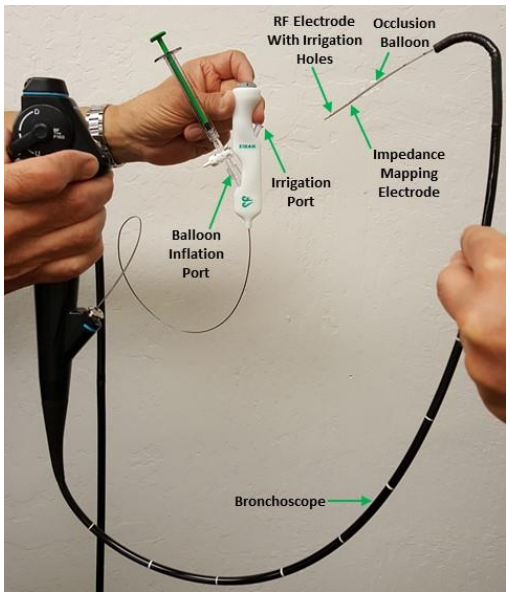

Figure 2 shows a close-up view of the catheter distal end. As shown in Fig. 3, the catheter profile was slim enough to easily path through the working channel of a commercially-available thin bronchoscope.

During RF energy delivery, the generator measured and displayed temperature, power, time, irrigation flow rate, monopolar impedance between the RF electrode and the neutral electrode and bipolar impedance between the RF and impedance electrodes.

B. Study Procedure

CT scans of the lungs were taken using a GE Lightspeed 64-slice CT scanner (General Electric, Massachusetts, USA) with inspiration held. Target bronchi were located and access path was planned. The target location was carefully chosen using the CT scans so that ablation volumes exceeding the size of a hypothetical 2 cm spherical nodule could be safely delivered. Multiple CT scans were taken to confirm RF electrode locations and to ensure sufficient clearance to pleura, or to other adjacent organs. These steps were taken to increase

animal safety and to minimize chances of complications, such as pneumothoraxes. For example, Fig. 4 shows an axial CT view of lower lung lobes with a sufficient clearance from the targeted RF electrode location (i.e. center of the 4 cm diameter circle) to the pleura. In this example, the RF energy settings were expected to produce a volume of approximately 4 cm in maximum diameter size. As such, a 4 cm diameter circle was drawn, centered on the targeted location of the RF electrode. An additional clearance distance of approximately 1.5 cm was verified to exist to the closest pleural surface. While the 1.5 cm clearance was chosen somewhat arbitrarily, it did work, as there were no pneumothorax complications in the study. Other clearances might have worked as well. Similar steps were employed to confirm sufficient clearance to adjacent organs in coronal and sagittal CT views.

Figure 4. CT axial view of the lower lobes illustrating sufficient clearance to pleural or diaphragm surfaces.

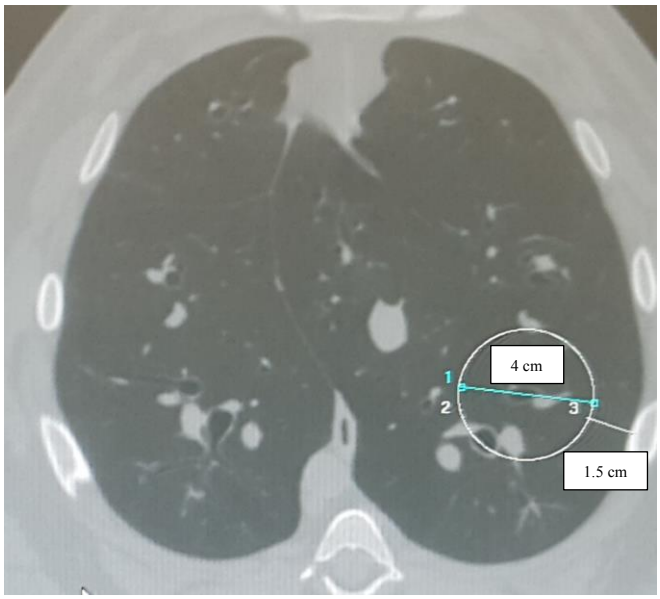

In other words, attention was paid to the clearance of the RF electrode with respect to the pleura and the diaphragm so that the expected ablation volumes would have inconsequential involvement of the pleura or of the diaphragm. A disposable 5-mm outer diameter bronchoscope (Ambu, Copenhagen, Denmark) with a 2.2 mm working channel was used to gain access to the target bronchi [9]. The catheter was tracked through the working channel and placed so that the ablation electrode reached the intended target location. The balloon was then deployed. A baseline bipolar impedance reading was taken with the catheter at the intended location. With the airway occluded by the balloon, vacuum suction was applied via the catheter irrigation holes to remove, at least partially some air from the targeted bronchus. This step improved the electrical contact between electrode and bronchial wall. Upon completion of air suction, the bipolar impedance decreased by about 10%, on average. Hypertonic saline was then released to further enhance electrode contact to the bronchial wall. After the bipolar impedance dropped further, to reach its pre-ablation target of about 200 Ω, delivery of RF energy was initiated.

C. Animal Study

Nine male, healthy Yucatan swine were treated with the RFA system. The study protocol was approved by the IACUC at Sutter Institute of Medical Research, Sacramento, CA. At the start of the study, animals weighed, on average 55.4±3.5 kg. The animals were kept under general anesthesia during the procedure. In all animals, the treatment sites consisted of one bronchus in the right upper lobe (RUL) and one bronchus in the right lower lobe (RLL). RF energy was delivered at power settings starting at 40 W and ramped up to 75 – 80 W. RF delivery durations were 6 min and 8 min at RUL and RLL, respectively. Hypertonic saline with a concentration of 23.4% was used for all animals except 1 animal, for which 5% saline was used. Flow of the HS irrigation was controlled by the proprietary algorithm at values between 0 – 12 ml/min so to maintain the sensed temperature within a range around 90°C. Three animals were survived to 1 week, another 3 animals to 4 weeks and the remaining 3 animals to 12 weeks. All animals were housed under professional observation for the duration of their survival. The study was completed with gross pathology of the lungs and surrounding structures and histology of the treatment sites. After animals were humanely sacrificed a limited postmortem gross necropsy examination was performed to evaluate the thoracic cavity and treatment sites in the lungs. The lungs were removed *en bloc*. For most animals, the lungs were perfused by gravity with 10% Neutral Buffered Formalin (NBF). For one animal, samples of the both upper and lower lung treatment sites were collected immediately after sacrifice and snap frozen in OCT media for cryotome sectioning and Nicotinamide Adenine Dinucleotide (NADH) viability staining using Nitro Blue Tetrazolium (NBT). In this animal, additional representative samples treatment sites were also collected in NBF. After adequate fixation the treatment sites were serially sectioned, photographed, and representative samples were obtained for histological evaluation. Tissues in cassettes were then routinely processed in graded alcohol, cleared in xylene and embedded in paraffin blocks. Paraffin blocks were sectioned on a microtome at 4-6 microns, mounted on glass slides and stained with Hematoxylin and Eosin (H&E) for routine light microscopic examination.

III. Results

All procedures were completed as planned. All animals survived for their respective planned study durations. Other than transient minor coughs, no complications were noted.

The ablation zones were well demarcated, separating necrotic from viable tissue. For the entire animal cohort, RUL ablations averaged 6 min, 67 W, 87°C, 86 Ω, 1.8 ml/min and 11 ml (total HS range 1 – 34 ml) for duration, power, temperature, monopolar impedance, flow rate and total infused HS volume, respectively. RLL ablations averaged 8 min, 66 W, 91°C, 89 Ω, 2.2 ml/min and 18 ml (total HS range 4 – 37 ml) for duration, power, temperature, monopolar impedance, flow rate and total infused HS volume, respectively. Over these nine animals, the total infused HS volume per lung (i.e. sum of RUL and RLL total HS volumes) ranged between 7 – 70 ml. Of note is the fact that no acute or

chronic adverse events occurred as a result of these levels of HS volume loading. Other than experimental variability (e.g. catheter location, proximity to blood vessels), there did not seem to be other causes for the differences between the RUL and RLL average parameters. RLL temperatures and flow rates were likely higher due to the increased RF delivery duration. At 1 week, the RUL ablation volumes had an average diameter of 3.2 cm. This average diameter decreased to 1.3 cm and to 1.1 cm after 4 weeks and 12 weeks survival intervals, respectively. At 1 week, the RLL ablation volumes had an average diameter of 3.8 cm. This average diameter decreased to 2.3 cm and to 1.6 cm after 4 weeks and 12 weeks survival intervals, respectively.

At 1 week, significantly large zones of necrotic tissue were observed in all ablations. The necrotic tissue was gradually replaced with fibrotic tissue. After 4-week survival, histology still showed residual necrotic tissue in all animals, but fibrotic replacement was already significant. At 12-week survival, the CT images indicated that the replacement was almost completed. Histopathology showed that at 12 weeks there was very little evidence of residual necrotic tissue.

Figure 5 shows an exemplar curve of the various parameters that are evaluated and controlled by the ablation algorithm. It can be seen that temperature curve (blue line) was maintained within a predefined target zone. The power was gradually ramped up from 40 to 80 W, at an approximate rate of 10 W/30 s. The flow of saline was controlled on and off by the system (gold line). The impedance (orange line) gradually fell over the duration of the procedure. The impedance spike, seen around $t = 25$ s on the plot, was likely caused by saline overheating.

Figure 5. Representative curve for Temperature, Impedance, Power and Flow during RFA.

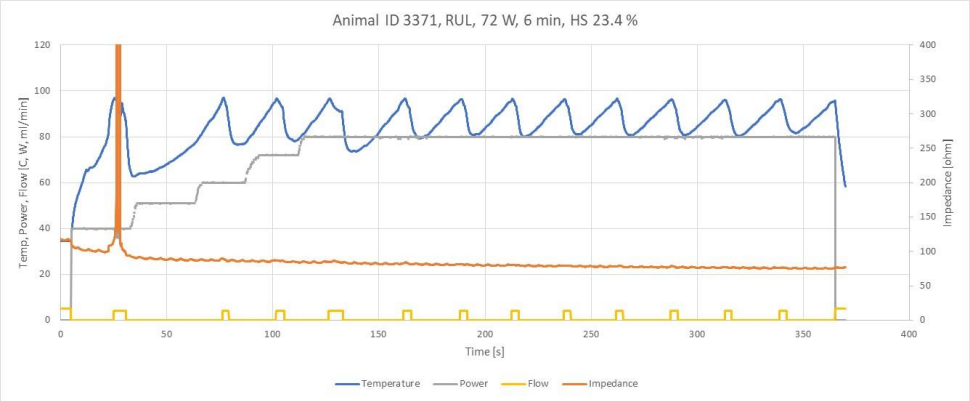

As shown in Fig. 6, CT scans taken at regular intervals revealed a gradual replacement of the ablated necrotic tissue with fibrotic tissue and the expansion of surrouding lung to fill the space left by the ablated region.

Figure 6. CT scan sequence of the RLL ablation for a representative animal over the 12 week period.

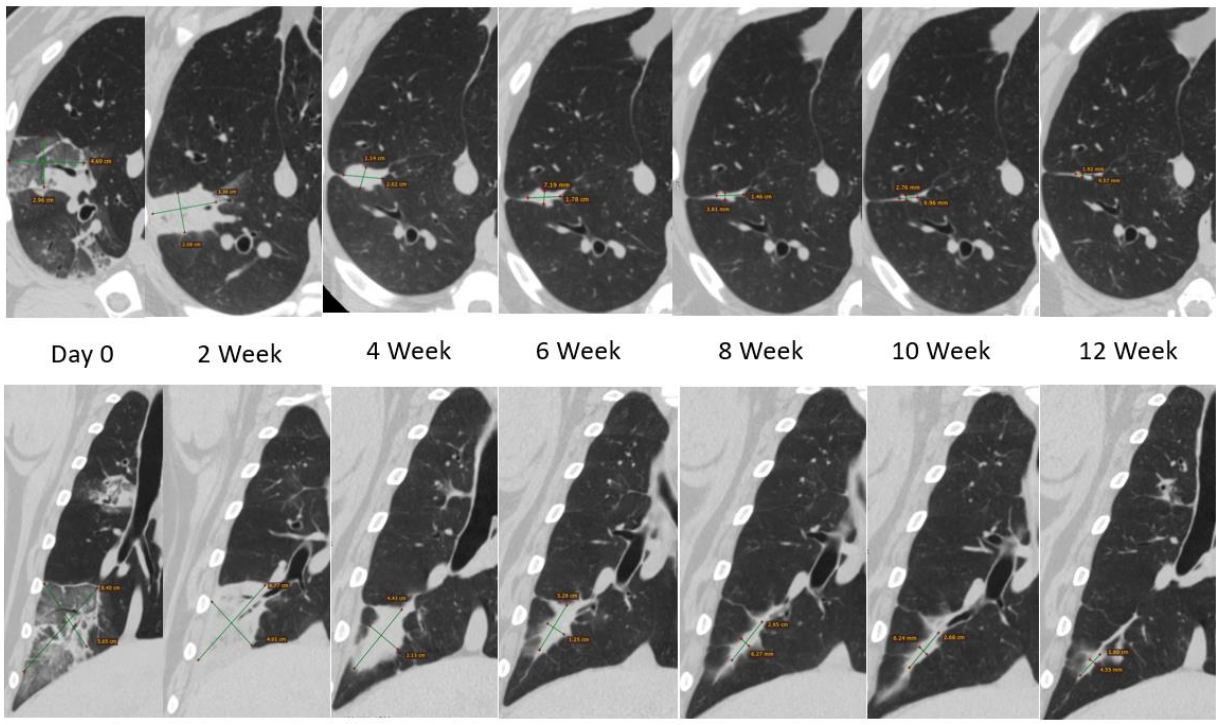

Figure 7. Gross slides of representative RLL ablations at the three time points. The inflammatory zone subsides with time and the necrotic region is gradually replaced by fibrotic tissues.

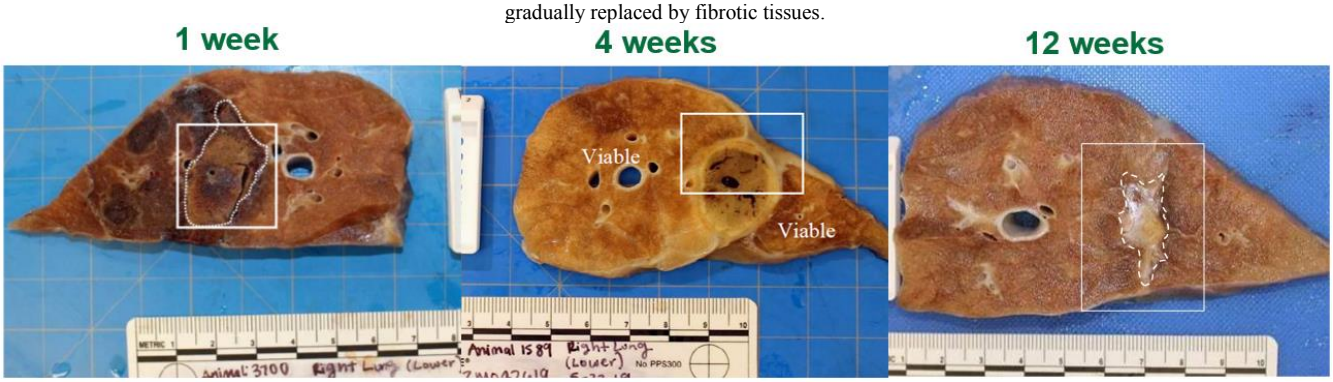

Figure 8. Histological sections of tissues in Fig. 7. At 1 week, a discrete zone of "heat fix" necrotic tissue (N) and surrounding viable (V) lung tissue was found. Gradual replacement by fibrotic tissue was seen at 4 weeks. At 12 weeks, only scar tissue was present.

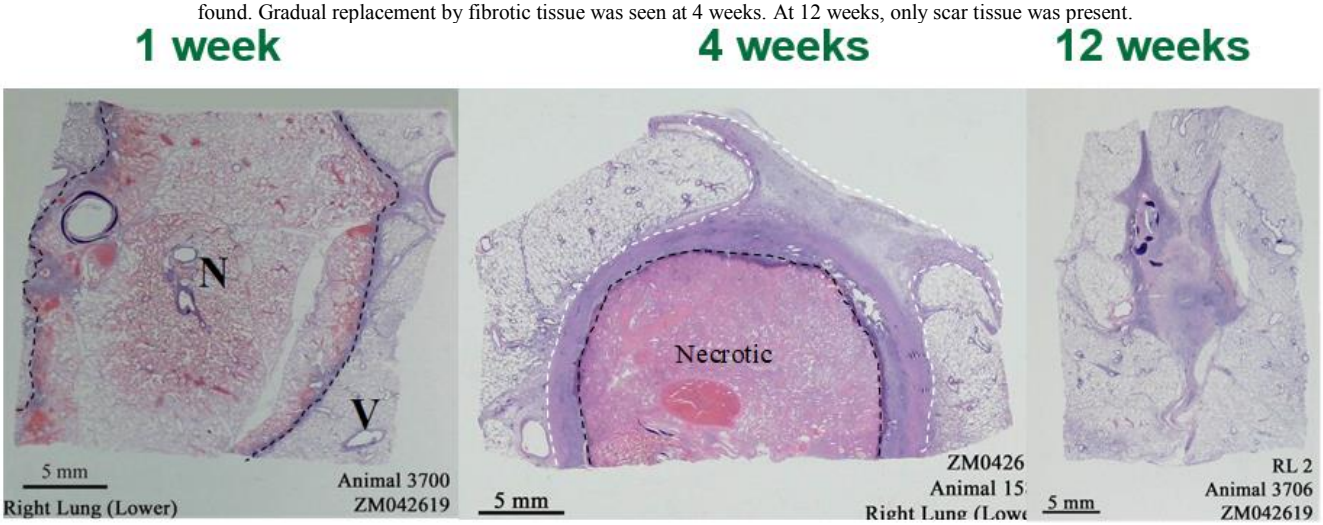

Cavitation was observed at 8 of the total 18 ablation locations. On average, cavities were less than 1 cm in size and healed completely by week #4. Only one ablation site displayed a residual cavity at 8 weeks which closed completely by week #10. None of these cavitation events resulted in any adverse events. A key factor in managing cavitation to secure animal safety was the preservation of sufficient clearance from the RF ablation electrode location to pleura or to major blood vessels or organs (e.g. diaphragm, heart, esophagus, etc.). At the end of survival period images of sections of the gross lung were taken (Fig. 7) and histology was performed on select representative slices of the ablation zone (Fig. 8).

At 1 week, the "heat fix" necrotic area could be seen surrounded by a zone of congestion and inflammation. At 4 weeks, there was consolidation of alveolar parenchyma distal to the treated airway and a fibrous encapsulation had started to form. The necrotic tissue seen at week one was being walled off from the surrounding healthy lung. The congestion and inflammation had resolved. At 12 weeks, the treated airway and associated parenchyma was mostly resorbed. Small remnants of collapsed cartilage and small airways occluded with fibrous scar tissue remained. The previous site of thermal necrosis has almost completely been resorbed and remodeled (contracted) by fibrous connective tissue.

In one animal, NADH staining was performed to determine if there were any viable cells left in the ablated zone. With this stain, the viable tissue stains blue, while the non-viable tissue does not pick up stain. Figure 9 shows NADH stained sections of the upper and lower lobe. No viable cells were detected in the clearly demarcated necrotic zone. This showed the ability of the system to produce large zones of uniform coagulative necrosis. Had a tumorous nodule been present within such zone, it would be expected that all its cancerous cells be rendered completely and uniformly non-viable.

Figure 9. NADH staining at 1 week showed a clearly demarcated necrotic zone with no living cells in both upper and lower lobe.

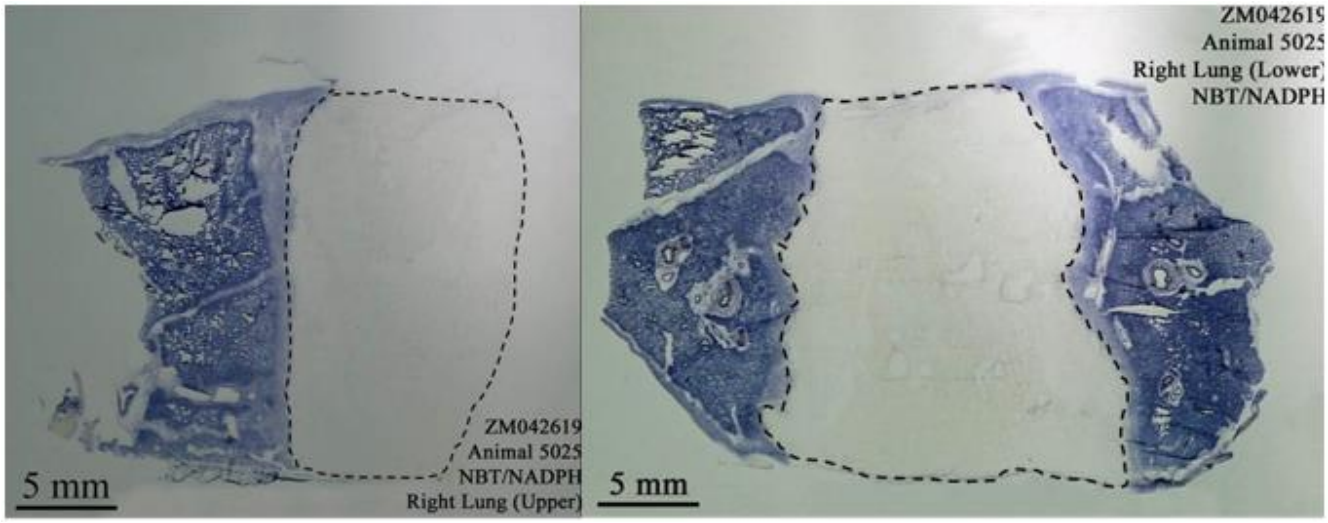

Figures 10 and 11 show the change in size of the ablation zone, over the 12-week interval, as measured from CT scans. As it can be seen, the majority of the resorption of the necrotic tissue happened over the first 4-6 weeks at a fast rate. After 6-8 weeks, mostly scar tissue remained, so there was minimal change in the size of the ablated region observed under CT.

Figure 10. RUL healing curves for three animals over a period of 12 weeks.

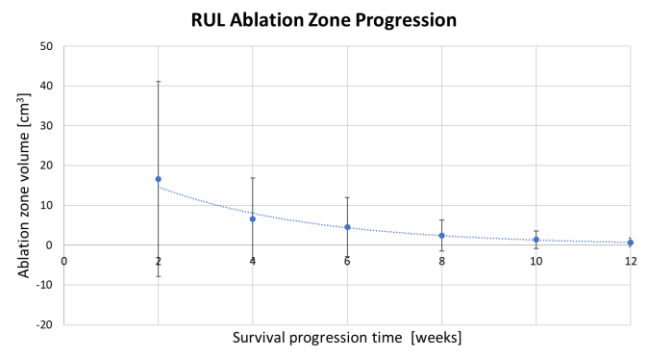

As indicated by the error bars, at all time points, ablation zone dimensions in both RUL and RLL regions displayed large variabilities from animal to animal. Given that the RF energy settings were similar in these three animals (e.g. RLL $RF_{Power\ range}$ = 62 – 64 W, $RF_{Temp\ Max\ range}$ = 89 – 91°C, $RF_{Duration}$ = 8 min), the large variability was likely caused by differences in catheter proximity to blood vessels and to other lung structures such as sublobular septa and fascias. Such sublobular structure seem to be more preponderant in swine than in humans.

IV. Conclusions

All safety endpoints were met for the study. No pneumothorax or unexpected changes were observed in the lung anatomy. No hemothorax, major bleeding or hemoptysis were observed (Table I). All blood chemistry and hematology values for all animals were in normal ranges after the treatment and stayed so through termination date.

Figure 11. RLL healing curves for three animals over a period of 12 weeks.

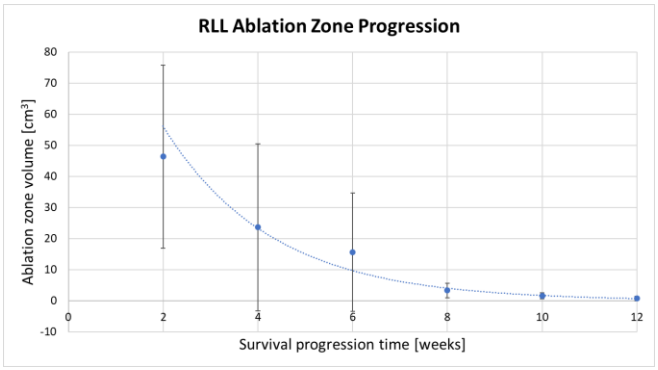

Specifically, in spite of our using irrigating saline of very elevated hypertonicity (i.e. 23.4%), the sodium (Na) levels did not show any significant changes at immediate post-ablation and at termination times vs. their pre-ablation values. This elevated hypertonicity did not result in acute or chronic adverse events up to total infused volumes of 70 ml/lung. Neutrophils and white blood cell count did not show signs of any systemic infections.

Individual ablation volumes displayed variability caused by specific catheter placement locations, proximity to large blood vessels and to pleura. However, the overall averages confirmed that ablation volumes were larger, on average, at higher energy settings (e.g. higher power or longer duration).

TABLE I. Summary of Adverse Events Occurring in Survival Cohort of Animals (9) Treated with Zidan RFA System.

Adverse Event	Frequency
Stroke/MI	0
Pneumonia	0
Cardiovascular/Respiratory Distress	0
Pneumothorax	0
Pleural Effusion	0
Pericardial Effusion	0
Infection	0
Unscheduled Death	0

In Yucatan swine, the treatment of lung tissue using this novel endobronchial RF ablation system was shown to be safe up to the end of the 12-week survival interval. No clinically adverse events occurred following treatment using this system. Animals vital signs, breathing patterns and their behavior were normal throughout the survival period. Their appetite was normal and they gained weight according to expectations. Figure 12 shows a schematic of the evolution of the treatment zone, as observed with our ablation system. The RF ablation created discrete areas of thermal coagulative necrosis which was initially encapsulated ("walled off") by a zone of organized fibrosis and subsequently completely replaced by fibrotic tissue. At 1 week post treatment, the necrotic ablation zone (brown) is an area of "heat fixed" thermal necrosis where the architecture of the lung tissue is "fixed" in position, but necrotic. Once the necrotic tissue is recognized by the host as a foreign body, an appropriate inflammatory response is elicited. The red rim around the necrotic tissue represents a zone of congestion. There is also a thin rim of early, organizing fibrous encapsulation represented in yellow. The surrounding (purple) lung tissue is collapsed, congested and variably edematous. At 1 month post treatment, the necrotic tissue (brown) has been recognized by the host as a foreign body and the appropriate inflammatory response has been elicited. The purple dots around the necrotic tissue represent a zone of foreign body inflammation. There is also a thin rim of early, organizing fibrous encapsulation represented in tan. The surrounding (purple) lung tissue is collapsed, congested and variably edematous. At 3 months post treatment, the treated airway and associated parenchyma is mostly resorbed. Small remnants of collapsed cartilage and small airways are occluded with fibrous scar tissue. The previous site of thermal necrosis has almost completely been resorbed and remodeled (contracted) by fibrous connective tissue. A thin linear streak of fibrous scar tissue remains.

Appropriate energy settings combined with suitable treatment locations (e.g. sufficient clearance to pleura, diaphragm, heart, esophagus) may result in safe and large volumes of uniform thermal coagulative necrosis. Further studies and optimization of treatment parameters may develop this technology into a mainstream therapy for potentially treating early-stage lung tumors in humans.

ACKNOWLEDGMENT

Catheters were built by AuST, West Valley City, UT. The RF generator, pump and cables were built by RBC Medical Innovations, Lenexa, KS.

REFERENCES

[1] "World Cancer Research Fund," [Online]. Available: www.wcrf.org. [Accessed 13 November 2018].

[2] T. Iishi, "Infusion of Hypertonic Saline into the Lung Parenchyma during Radiofrequency Ablation of the Lungs with Multitined Expandable Electrodes: Results Using Porcine Model," *Acta Medica Okayama*, vol. 63, no. 3, pp. 137-144, 2009.

[3] C.-K. Chen, "Image-guided lung tumor ablation: Principle, technique, and current status," *J. Chinese Med. Assoc.*, vol. 76, pp. 303-311, 2013.

[4] T. S. Kim, H. K. Lim and H. Kim, "Excessive hyperthermic necrosis of a pulmonary lobe after hypertonic saline-enhanced monopolar radiofrequency ablation," *Cardiovasc. Intervent. Radiol.*, vol. 29(1), pp. 160-3, 2006.

[5] D. Panescu, J. G. Whayne, S. D. Fleischman, M. S. Mirotznik, D. K. Swanson and J. G. Webster, "Three-dimensional finite element analysis of current density and of thermal profiles during radiofrequency ablation," *IEEE Trans. Biomed. Eng.,* vol. 42(9), pp. 879–890, 1995.

[6] M. Kashima, "Complications After 1000 Lung Radiofrequency Ablation Sessions in 420 Patients: A Single Center's Experience," *Vasc. Interv. Radiol.*, vol. 197(4), pp. 577-580, 2011.

[7] N. Bi, K. Shedden, X. Zheng and F. S. Kong, "Comparison of the Effectiveness of Radiofrequency Ablation With Stereotactic Body Radiation Therapy in Inoperable Stage I Non-Small Cell Lung Cancer: A Systemic Review and Pooled Analysis," *Int. J. Radiat. Oncol. Biol. Phys.*, vol. 95(5), pp. 1378-1390, 2016.

[8] J. M. Lee, "Saline-Enhanced Radiofrequency Thermal Ablation of the Lung: A Feasibility Study in Rabbits," *Korean J. Radiol.*, vol. 3(4), pp. 245-253, 2002.

[9] K. Yoneda, S. Li, F. Herth, M. Gelfand, S. Raina and D. Panescu, "Early preclinical experience with a novel RF ablation system for lung cancer treatment," *IEEE Eng. Med. Biol. Soc.*, vol. 41, pp. 174-180, 2019.

[10] Ambu, [Online]. Available: www.ambu.com.

[11] FDA Drug Shortages, https://www.accessdata.fda.gov/scripts/drugshortages/dsp_ActiveIngredientDetails.cfm?AI=Sodium+Chloride+23.4per+Injection&st=c&tab=tabs-4&panels=1

Figure 12. Illustration of typical treatment zone evolution: 1 week, 1 month and 3 months post-treatment.

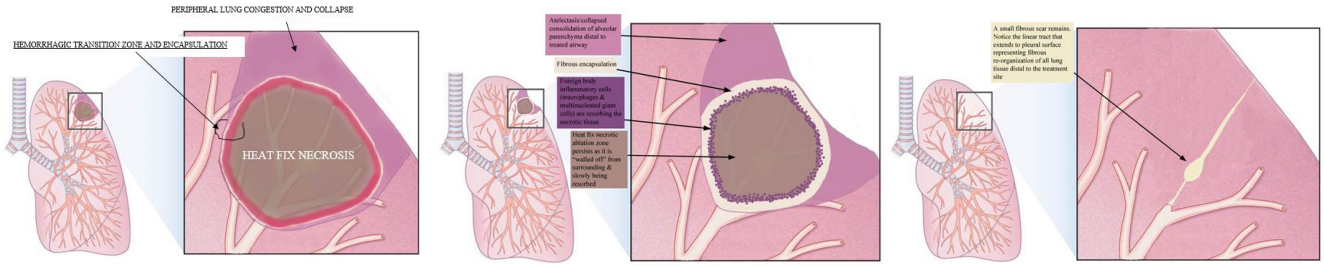

1 week 1 month 3 months